The characteristics of clusters of weather and extreme climate events in China during the past 50 years*

Yang Ping (杨 萍)[a)b)], Hou Wei(侯 威)[b)], and Feng Guo-Lin(封国林)[b)†]

[a)] *Institute of Urban Meteorology, China Metrology Administration, Beijing* 100089, *China*

[b)] *Laboratory for Climate Studies, China Meteorological Administration, Beijing* 100081, *China*

(Received 14 June 2011; revised manuscript received 17 August 2011)

The pick-up algorithm by the k-th order cluster for the closest distance is used in the fields of weather and climactic events, and the technical terms clustered index and high clustered region are defined to investigate their temporal and spatial distribution characteristics in China during the past 50 years. The results show that the contribution of extreme high-temperature event clusters changed in the period from the 1960s to the 1970s, and its strength was enhanced. On the other hand, the decreasing trend in the clusters of low-temperature extremes can be taken as a signal for warmer winters to follow in the decadal time scale. Torrential rain and heavy rainfall clusters have both been lessened in the past 50 years, and have different cluster characteristics because of their definitions. Regions with high clustered indexes are concentrated in southern China. The spatial evolution of the heavy rainfall clusters reveals that clustered heavy rainfall has played an important role in the rain-belt pattern over China during the last 50 years.

Keywords: extreme event, clusters, decadal clustered index

PACS: 92.60.Wc **DOI:** 10.1088/1674-1056/21/1/019201

1. Introduction

Under the background of climactic warming, extreme weather and climactic events occur more frequently and more widely and result in more damage.[1−4] These events appear to have an obvious multi-occurrence characteristic in the global scope. Multi-occurrence is an important characteristic of extreme climactic events and is also called a cluster, whose features can be described by cluster analysis. If an extreme climactic event is persistent over a long time and is widespread, it is observed by many observation stations and influenced by many weather patterns. When extreme climactic conditions last for a long time, for example when durative precipitation is continuous for several weeks in the rainy season, it is called a persistent extreme climate event.[5−7] When this occurs over a region, it is called a cluster extreme climate event.[8−11] In other words, the extreme event observed frequently in one observation state is not randomly scattered in the whole area but concentrated in a certain region. For example, many regions in southern China suffered disastrous freezing conditions from January to early February 2008.[12] The study of persistent extreme climate events over a long time scale is difficult because of limited data. However, a cluster extreme event may be considered from its spatial identity, and whether a cluster region can be detected using an objective method is a very interesting topic to study.

Although an extreme climate event cannot be considered as a point, a single station, where an extreme climate event is observed, can be taken as a random point scattered in a wide spatial area. Similarly, many natural disasters, such as earthquakes and volcano eruptions, can be seen as randomly scattered spatial points.[13−15] Generally, the distribution of the points is not uniform in space, and is dense over some regions but sparse over others. Cluster extreme climate events occur in regions with serried points.[16,17] Many researchers have investigated cluster point detection approaches, such as the density-based method, wavelet transformation and the concentration ratio in-

*Project supported by the National Natural Science Foundation of China (Grant Nos. 41005043 and 41105033), the National Basic Research Program of China (Grant No. 2012CB955901), and the National Science and Technology Ministry, China (Grant Nos. 2007BAC29B01 and 2007BAC03A01).

†Corresponding author. E-mail: Fenggl@cma.gov.cn

© 2012 Chinese Physical Society and IOP Publishing Ltd

dex. However, many of these methods need to select the judgment parameters subjectively.[18] In the algorithm of k-th order distance cluster mining, the k-th nearest-neighbour (k-NN) concept is transplanted from the spatial point process theory. Based on this concept, a two-dimensional (2D) data set comprised of cluster points and sparse points in a certain area can be transformed into a one-dimensional function of point distribution mixing intensity. Using the expectation-maximization (EM) algorithm to decompose the intensity function, the clustered points can be identified.

Based on the k-NN algorithm and its application, the validity of the method for studying clustered extreme events is tested and verified in this paper. In particular, characterizing clustered temperatures and extreme precipitation events is analyzed. The concept of a clustered index is introduced to measure the temporal evolvement and spatial change of weather and extreme climate events in the decadal scale.

2. Algorithms

2.1. The basic theory of the distribution of k-NN

Given a point s_i in the 2D Poisson point set Y, its spatial probability distribution function (PDF) of the k-th nearest-distance W_k can be acquired from distribution functions with 0, 1, 2, ..., $k-1$ points inside a radius of x, and the distance between s_i and its k-NN is within x. For $x \in [0, \infty)$,

$$\begin{aligned} P(W_k \geq x) &= \sum_{m=0}^{k-1} \frac{\mathrm{e}^{-\lambda\pi x^2}(\lambda\pi x^2)^m}{m!} \\ &= 1 - G_{W_k}(x), \end{aligned} \tag{1}$$

where k is the parameter referring to the distance order, $G_{W_k}(x)$ is the cumulative distribution function of W_k, and λ is the rate of the Poisson point set. If W_k is larger than x, there must be one of 0, 1, 2, ..., $k-1$ points in the circle. The $g_{W_k}(x)$ is the derivative of $G_{W_k}(x)$,

$$g_{W_k}(k, \lambda) = \frac{\mathrm{e}^{-\lambda\pi x^2} 2(\lambda\pi)^k x^{2k-1}}{(k-1)!}. \tag{2}$$

According to the definition of the distribution density function, it is a $\Gamma(k, \lambda\pi)$ function, as $Y \sim \Gamma(k, \lambda\pi)$, where $Y = (W_k)^2$.

In the research, the noise and cluster can be represented as two superimposed Poisson processes with different rates. In this way, the bimodal PDF of W_k can be expressed as

$$W_k \sim p\Gamma^{1/2}(k, \lambda_1\pi) + (1-p)\Gamma^{1/2}(k, \lambda_2\pi), \tag{3}$$

where p represents the proportion coefficient, λ_1 and λ_2 are the rates for two different processes, and k is the distance order.

2.2. The expectation-maximization algorithm to evaluate parameters

Byers and Raftery[19] proposed an EM algorithm to estimate the intensities of the feature event (λ_1) and the noise event (λ_2) when two point processes are superimposed in a restricted region. A summary of the main idea is given in the following.

For region S containing two Poisson processes with different intensities, the PDF of W_k can be treated as a mixture PDF with different intensities. It is expressed as

$$W_k \sim p g_{W_k}(k, \lambda_1) + (1-p) g_{W_k}(k, \lambda_2), \tag{4}$$

where p is the proportional coefficient, λ_1 and λ_2 are the intensities of the two distributions, respectively, and k is the distance order parameter. A simple application of the EM algorithm is to estimate parameters λ_1, λ_2 and p, which characterize the postulated distribution of W_k. The EM algorithm includes two steps, the E step and the M step. The E step of the algorithm consists of

$$E(\hat{\delta}_i^{(t+1)}) = \frac{\hat{p}^{(t)} g_{W_k}(k; \hat{\lambda}_1^{(t)})}{\hat{p}^{(t)} g_{W_k}(k; \hat{\lambda}_1^{(t)}) + (1-\hat{p}^{(t)}) g_{W_k}(k; \hat{\lambda}_2^{(t)})}, \tag{5}$$

while the M step is composed of

$$\begin{aligned} \hat{\lambda}_1^{(t+1)} &= \frac{k \sum_{i=1}^{n} \hat{\delta}_i^{(t+1)}}{\pi \sum_{i=1}^{n} W_{k,i}^2 \hat{\delta}_i^{(t+1)}}, \\ \hat{\lambda}_2^{(t+1)} &= \frac{k \sum_{i=1}^{n} (1 - \hat{\delta}_i^{(t+1)})}{\pi \sum_{i=1}^{n} W_{k,i}^2 (1 - \hat{\delta}_i^{(t+1)})}, \\ \hat{p}^{(t+1)} &= \sum_{i=1}^{n} \hat{\delta}_i^{(t+1)} \Big/ n, \end{aligned} \tag{6}$$

where n is the number of points, $W_{k,i}$ is the k-th nearest distance of event q_i (i = 1, 2, ..., n) and t is the number of iterations. If λ_1 is defined as the quantity representing the cluster, then events with $\hat{\delta}_i^{(t+1)} \geq 0.5$ belong to the cluster, and events with $\hat{\delta}_i^{(t+1)} < 0.5$ can be viewed as noise.

3. The delineation and detection of clustered extreme climate events

The value of k and its influence on method applicability has been discussed by Pei *et al.*,[20,21] and it was found that k is a key parameter in estimating the clusters. A moderate value of k can reduce the error rate in the algorithm. Much work has been done by Yang *et al.*[22] to estimate the applicability of the method. Besides the distance order k, two other parameters – the total number of sample n and the ratio of the clustered pint intensity to the sparse point intensity R – are very important to the result. So R is used to quantify the applicability of the EM algorithm. Much research has been done on the value settings for different data sets to extend its applicability.

Despite the fact that the locations of the points of the extreme events are certain, the frequency and the intensity of the extreme events are different. Denseness can be increased in a region if the frequency and intensity characteristics are considered. This is in favour of the detection of strong extreme climate events. The effectiveness of the temperature and precipitation extreme events defined in different ways is examined, and it is revealed that the algorithm is applicable to the clustered weather and extreme climate events, especially in momentous extreme events.[23] These results provide a solid background of theory and algorithms for studying cluster extreme climate events.

3.1. The regional data

Background extreme events refer to slight events that occur with low weighing coefficients. Clustered extreme events refer to a swarm of extreme climate events occurring with high weighing coefficients.[23] With these definitions, background and clustered events can be seen as two overlaid spatial processes with different intensities. As we know, meteorological stations are not uniformly distributed in China, especially in western China, so the regions involved in this paper are mostly in eastern China. The regions with sparse stations belonging to the provinces in the western part, such as Tibet, Xinjiang and Inner Mongolia, are not included to reduce the influence of uneven distribution on the calculations.

The data set from a total of 740 stations was collected and processed by the National Meteorological Centre of the China Meteorological Administration and is used in this paper. The data set is composed of daily maximum/minimum temperatures covering the period from 1960 to 2005, and precipitation covering the period from 1960 to 2006. After eliminating the stations with incomplete data, there were 426 stations left to provide the temperature data set and 437 to provide the precipitation data set. The distributions of the stations are shown in Fig. 1.

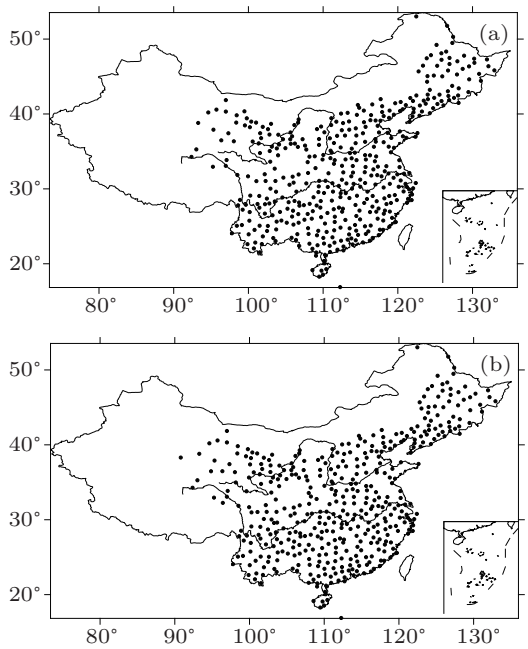


Fig. 1. The distribution of the meteorological stations providing (a) temperature and (b) precipitation data sets.

3.2. Detection of clusters

Based on the k-NN method and the definition of extreme climate events, clustered extreme climate events have been detected year after year. The detection process for delineating the clusters is summarized in Fig. 2.

The high-temperature events observed every summer by 426 observatory stations over China from 1960 to 2005 are taken as an example to explain the detection process of the extreme event cluster. For a randomly chosen station, the daily maximum temperature data from 1960 to 2005 are ordered ascendingly. A case with a temperature higher than the threshold value (higher than 99% of the data in the set) can be considered as a summer high-temperature event, and the frequency of high-temperature events in each station is summed up. The weight with a fixed ratio is given to the clustered point set and is made to approach the utmost. Using the k-th nearest-neighbour

cluster mining algorithm, which originates from the spatial process theory, the clustered maximum temperature events can be picked up, and the clustered distribution of the data set can be established every year from 1960 to 2005.

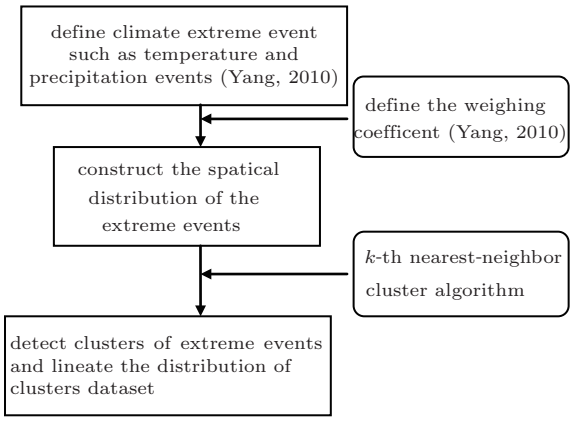


Fig. 2. A process chart of clustered extreme event detection.

Take the year 2003 for example, the temperature distributions and the clustered extreme temperature events are shown in Fig. 3(a). From

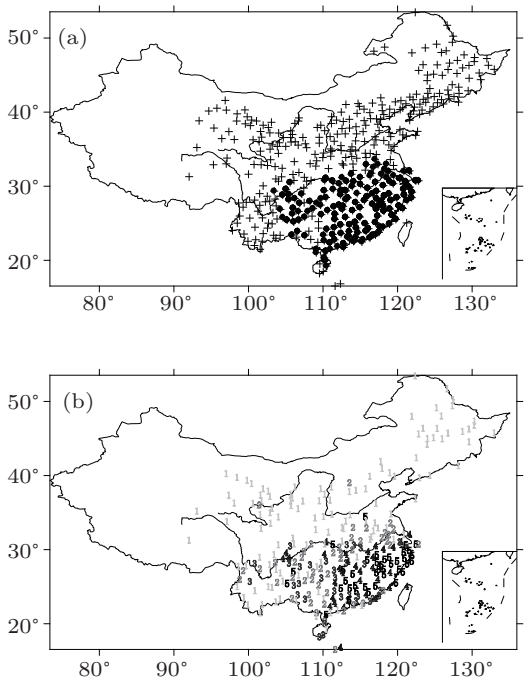


Fig. 3. The features of extreme temperature events observed by stations over China in 2003: (a) clustered distribution, where the crosses and dots represent the stations where the temperature and clustered extreme temperature events are observed, respectively; and (b) weighted distribution, where the numbers represent the weights of the stations.

Fig. 3(a), we notice that the extreme temperature events (crosses) take place over almost the whole of eastern China, while the clusters of extreme events (dots) concentrate in southern China. The cluster extreme event is clearly detected and picked out. The distribution of the weighing coefficients for the stations is given in Fig. 3(b). Comparing Fig. 3(a) with Fig. 3(b), it is clear that the stations with high weighing coefficients or those remaining in the high density area are depicted as the clustered events. It is shown that this method can be used to evaluate the clusters reasonably well, and that subjectivity is reduced in the detecting process.

4. Temporal and spatial variations of clustered extreme events

4.1. Temporal variety and trends

The interannual variations in different kinds of clustered extreme events, including high-temperature extreme events, low-temperature extreme events, torrential rain events and strong precipitation events, are shown in Fig. 4. The dashed lines represent their linear trends, while the solid lines refer to the moving averages, which are averaged over 10 years for the extreme temperature events and 7 years for extreme precipitation.

Almost no obvious trend is found for the clustered high-temperature extreme events (Fig. 4(a)), but it is distinguished in the divided periods. The moving average shows that there is a transitional period for the clustered high-temperature extreme events in the late 1970s, which is consistent with the mutation of the atmosphere-ocean system over the northern Pacific Ocean.[24] After the turning point, the declining trend changes to an ascending one, particularly after the 1990s. The clusters of low-temperature extreme events (Fig. 4(b)) go down, in contrast to those of the high-temperature extreme events, which is in accordance with the point suggested by Karls *et al.*[25] The turning lies in the late 1970s, 5 years ahead of the break time for the warmer winter over China. It is suggested that the clusters of low-temperature extreme events appear to be a weak trend, which implies that a warm winter period is coming. This feature is similar to the results given in Refs. [25]–[28]. The clustered torrential rain event appears as characteristic of

the interim change (Fig. 4(c)), with a strong cluster period from 1960 to 1975 but a weak cluster period until the early 1980s. It has an alternating variation in the 1990s and then becomes a lessened trend until the present day. A feeble decrease in the clustered heavy precipitation event is shown in Fig. 4(d), almost without any decadal variation phase. This may imply that the clusters of heavy precipitation are dominated by interannual oscillation. A 5 year period has been found in the power spectral analysis for the clusters of heavy precipitation events, which nearly accords with the El Niño-Southern Oscillation cycle. The difference in the characteristics between the clusters of the torrential rain event and the heavy rain event is probably attributed to the difference in definition between these two events.

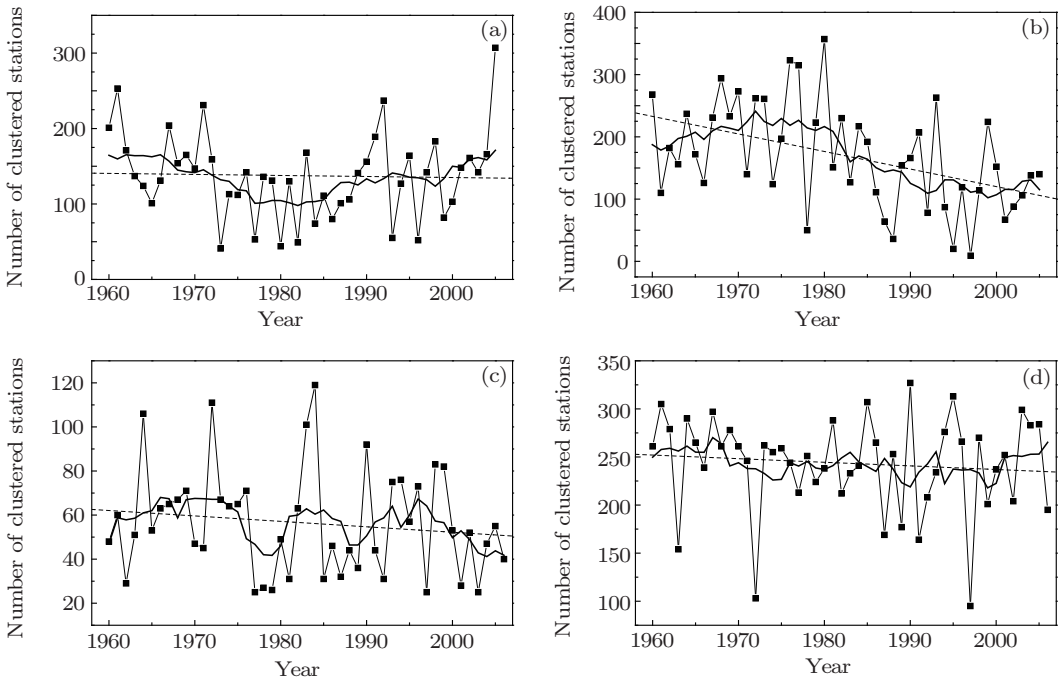


Fig. 4. The interannual variability results of clustered (a) high-temperature extreme events, (b) low-temperature extreme events, (c) torrential rain events and (d) heavy precipitation events.

4.2. Spatial evolution and trends

In this part, the k-NN method and the related theory introduced in the preamble are used to deal with the clusters of extreme events. The decadal clustered index (DCI) is defined, and the clustered events are divided into two stages according to the DCI. Then the decadal spatial evolutions of the clustered extreme climate events for the past 50 years in China will be discussed.

The definition of P_{DCI} (see Eq. (7)) is based on the results of the interannual change revealed from the k-th nearest-neighbour method, and the strength values of the clusters on different time scales are delineated by a unified formula based on the numerical statistic method. The clustered decadal variation of the extreme climate events can be evaluated quantificationally. The P_{DCI} is presented as

$$P_{\mathrm{DCI}} = \frac{n_M/M}{n_L/L} \times \frac{n_M}{n_{\mathrm{sum}}/N}, \tag{7}$$

where L is the length of the data series, n_L represents the frequency in the L series, M is the decadal length, n_M is the frequency in the M series, N is the total number of the stations and n_{sum} is the sum of the frequency of all clustered stations among the M series. P_{DCI} with a high value belongs to the low probability event. In this paper, a high-value area with a cumulative probability above 85% is estimated to be the first stage area, while that above 70% is in the second stage area. The threshold values of the different extreme climate events are listed in Table 1.

Table 1. The threshold values of different extreme climate events.

Threshold	Temperature extremes	Torrential rain	Heavy rainfall
First stair	2.2	4.0	1.8
Second stair	1.6	2.5	1.4

4.2.1. Extreme temperature events

The spatial distributions of the decadal clustered extreme temperature events with high values are shown in Fig. 5. Figure 5(a) shows the high-temperature extreme events and (b) exhibits the low-temperature extreme events.

It can be seen in Fig. 5(a) that the distributions of P_{DCI} for the high-temperature extreme events are disparate in different decadal periods. In the 1960s, the high value of P_{DCI} lies in the region from the Huanghuai area to the Jianghuai area, and even extends southward. Another high cluster region is located south of the Yangtze River, although the strength of the clustered high-temperature extreme events is somewhat weaker compared with that in the Jianghuai area. In the 1970s, a high P_{DCI} value vanishes in the northern and central regions of China, but appears over northeastern China and in the upper-middle reaches of the Yellow River. After that, it has been noticed that the cluster strength evidently falls off. Apart from a few areas in southern and northeastern China, the high values only remain in western China, and some of the first stage areas turn up in Yunnan in the 1980s. The distribution of P_{DCI} shows an increase from south to north over the region south of the Yangtze River. Obvious first-stage cluster high value areas exist over the upper and lower reaches of the Yangtze River and a few high-value areas in northern China in the 1990s. In the early 2000s, the areas with high P_{DCI} values show a leaping augment from south to north. If the location shift of the cluster high P_{DCI} value area is considered, it can be revealed that its migration path is first from east to west along the latitude and then from south to north along the longitude. Its strength is weakened at the beginning and then turns from weaker to stronger.

The features of low-temperature extreme events are given in Fig. 5(b). It is found that the high P_{DCI} values concentrate in the eastern coastal areas and north of the Yangtze River in the 1960s. In the 1970s, the main areas with high cluster indexes are located in the southwestern part of southern China. Apart from some scattered areas with second-stage cluster values, almost no first-stage cluster high value area can be found in the 1980s. In the 1990s, the high cluster index values are mainly distributed over the upper and middle reaches of the Yangtze River and the Yellow River. At the beginning of the new century, a pattern with a high P_{DCI} value emerges over both southern and northeastern China, while one with a low value appears over the region between them. In fact, northern, northeastern and southern China are the high cluster areas of the low-temperature extreme events in the period. Zhang and Li[29] suggested that the colder winter focused in western China in the 1960s and appeared to concentrate in southern and southwestern China in the 1970s. The cluster of the low-temperature extreme events in the 1960s is not very clear in Fig. 5(b), because the western region is excluded from the computation in this paper. However, it is still consistent with what Zhang *et al.*[29] pointed out in the 1970s. The result indicates that the increase in clustered low-temperature extreme events makes an important, maybe dominant contribution to a colder climate in the decadal time scale.

The evolution of the clustered extreme temperature events illustrates that the clusters of the low-temperature extreme events are narrowed in a smaller scope from the 1960s to the 1990s. The occurrence of low-temperature extreme events with high P_{DCI} values is almost fastened in southern China, particularly in the 1980s and the 1990s, in which a relatively high mean temperature and a high extreme low temperature exist. Combined with a distinct break that happened after 2000, the abroad clustered area of extreme temperature events shows up again over northern China. Meanwhile, the areas of clustered high-temperature extreme events increase, and their strength is enhanced. Further study is needed to ascertain whether this implies a restructuring of the climate state in China.[30]

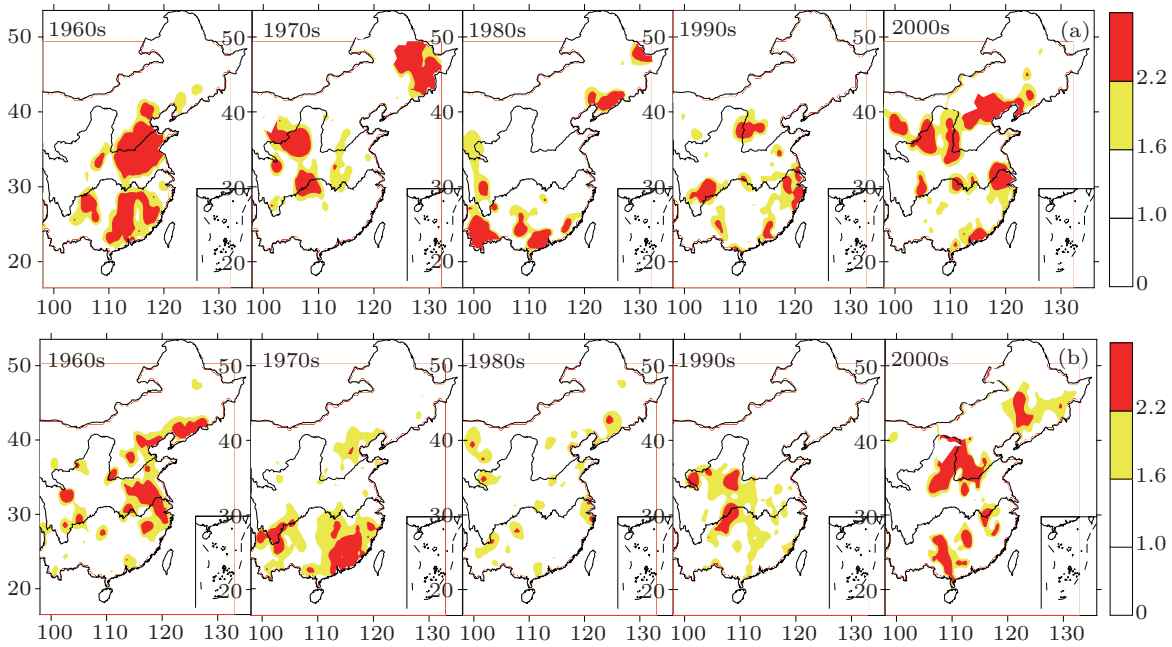


Fig. 5. (colour online) Distributions of (a) high-temperature and (b) low-temperature extreme events with high values of decadal cluster index. The fuscous shadows represent the first-stage areas with a cumulative probability above 85%, while the light ones denote the second-stage areas with a cumulative probability above 70%.

4.2.2. Extreme precipitation events

The decadal spatial distributions of the extreme precipitation events with high clustered index values are shown in Fig. 6. Torrential rain events and strong precipitation events are shown in Figs. 6(a) and (b), respectively.

According to their coverage areas, the torrential rain event clusters are sorted into primary and secondary clustered regions. It is indicated in Fig. 6 that the primary cluster stays dominantly over the coast of southeastern China in the 1960s and moves to southwestern China in the 1970s. During the 1980s, it appears in the Yellow River and the Huaihe River drainage areas, then comes back to the south in the 1990s, and shifts to the northwest in the 2000s, looking like a clockwise-moving trace in the areas south of the Yangtze River basin. On the other hand, the secondary clustered area seems to display a reversed moving pattern. In other words, the high value areas of the clustered torrential rain concentrate in the area south of the Yangtze River, which is likely to be related to the definition of the torrential rain. The rainfall with precipitation much more than 100 mm will have a lighter influence over the middle and low reaches of the Yangtze River than that over northeastern and northern China.[31]

Similarly, it is concerned to the high cluster region of heavy rainfall, as shown in Fig. 6(b). The high cluster region lies in northern and northeastern China in the 1960s. It is mainly located in the upper stream of the Yangtze River and the middle reaches of the Yellow River, along with the southwest-to-northeast pattern in the 1970s. After this, it appears in the Yangtze River drainage area in the 1980s, and goes down south to the low reaches of the Yangtze River. After 2000, it demonstrates a pattern with a high distribution in northern and southern China, but a few clusters are in the middle. In this period, the heavy rainfall clustered area focuses in the region south of the Yangtze River, and there is almost no high clustered value found in northern China. This evolution of heavy rainfall is similar to the rain-belt pattern over China.[32] It indicates that the decadal change in clustered heavy rainfall may play an important role in forming the rain-belt pattern over China.

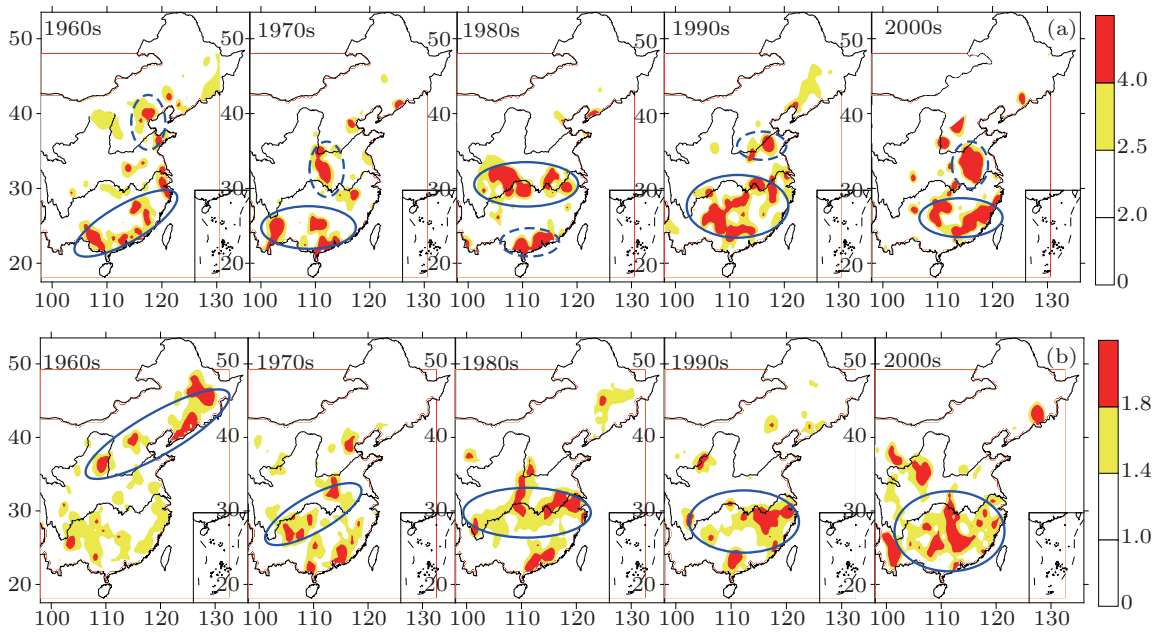


Fig. 6. (colour online) Distributions of (a) rainstorms (the solid lines show major cluster areas, while the broken lines show secondary cluster areas) and (b) strong precipitation events (solid lines show large cluster areas) with high values of decadal cluster index. In the figures, the fuscous shadow represents the first high value, while the light one shows the second high value.

5. Conclusions

Much of the research on extreme weather events is generally confined to statistical meteorological elements. Studying clusters of extreme weather events is a new and important topic. However, its quantitative analysis and detection method, and the related theories, still need to be studied further in the future.

The two main types of cluster definitions, temporal and spatial clusters, are proposed in this paper. Based on the k-th nearest-neighbour method of the clustered point extraction algorithm and the related theoretical research results, an approach to the detection of clustered extreme events is presented in this paper to find the characteristics of clustered extreme events in China.

Through data analysis, we find that the cluster of low-temperature extreme events in winter has decreased obviously in the last 50 years, while the cluster of high-temperature extreme events in summer shows an increasing trend. A remarkable result is that the weakening trend of the clusters of low-temperature extremes in the decadal scale may be a signal implying the arrival of warmer winters. Clusters of torrential and heavy rain have shown a lessened trend in the past 50 years, with distinct periods of oscillation. The difference between the clusters of torrential and heavy rain is probably due to the difference in the definition of these two events.

The spatial distributions of extreme temperature events present various features in different periods. There is a disparate difference in the spatial state between the 1960s and the 1970s. The increase in the P_{DCI} index of the low-temperature extreme events is unlikely to be a main contribution to the decadal cold background in the 1970s. The spatial evolution of the torrential rain event clusters behaves as a concentrated location in southern China. But the state of the cluster areas of heavy rainfall is consistent with that of the rain-belt pattern over China during the summer season. It therefore seems that the clustered heavy rainfall plays an important role in the formation of the rain-belt pattern over China.

References

[1] Alexander L V, Tapper N, Zhang X B, Fowler H J, Tebaldi C and Lynch A 2009 *Int. J. Climatol.* **29** 317

[2] Easterling D R, Evans J L, Groisman P Y, Karl T R, Kunkel K E and Ambenje P 2000 *Bull. Amer. Meteor. Soc.* **81** 417

[3] Ester M, Kriegel H P, Sander J and Xu X W 1996 *Proceedings of the Second International Conference on Knowledge Discovery and Data Mining* (Porland: Oregon) p. 324

[4] Jones P D, Osborn T J and Briffa K R 1997 *J. Climate.* **10** 2548

[5] Yan Z W, Jones P D, Davies T D, Moberg A, Bergstrom H, Camuffo D, Cocheo C, Maugeri M, Demaree G, Verhoeve T, Thoen E, Barriendos M, Rodriguez R, Martin-Vide J and Yang C 2002 *Climatic Change* **53** 355

[6] Qian W, Fu J and Yan Z 2007 *Geo. Res. Lett.* 34 L11705

[7] Choi G D, Collins D, Ren G Y, Trewin B, Fukuda Y, Afzaai M, Pianmama T, Gomboluudev P, Huong P, Lias N, Kwon W, Boo K, Cha Y and Zhou Y 2009 *Int. J. Climatol.* **29** 1906

[8] Ding Y H, Wang Z Y, Song Y F and Zhang J 2008 *Acta Meteorol. Sin.* **66** 808 (in Chinese)

[9] Qian Z H, Feng G L and Gong Z Q 2010 *Acta Phys. Sin.* **59** 7498 (in Chinese)

[10] Gong Z Q and Feng G L 2008 *Acta Phys. Sin.* **57** 3920 (in Chinese)

[11] Feng G L, Yang J, Wang S Q, Hou W and Zhi R 2009 *Acta Meteorol. Sin.* **67** 61 (in Chinese)

[12] Tao S Y, Wei J, Sun J H and Zhao S X 2009 *Meteorological Monthly* **35** 3 (in Chinese)

[13] Brimicombe A J 2003 *Lecture Notes in Computer Science* **2669** 1

[14] Steenberghen T, Dufays T, Thomas I and Flahaut B 2004 *Int. J. Geogr. Inf. Sci.* **18** 169

[15] Ogata Y 2001 *J. Geophys. Res.* **106** 8729

[16] Ren G Y, Chu Z Y and Chen Z H 2007 *Geo. Res. Lett.* **34** 1

[17] Ren G Y, Guo J, Xu Z M, Chu Z Y, Zhang L, Zhou X K, Li Q X and Liu X N 2005 *Acta Meteorol. Sin.* **63** 942 (in Chinese)

[18] Pei T, Zhou C H, Yang M, Luo J C and Li Q L 2004 *Acta Seismogica Sin.* **26** 53 (in Chinese)

[19] Byers S D and Raftery A E 1998 *J. Am. Stat. Assoc.* **93** 577

[20] Pei T, Zhu A X, Zhou C H, Li B L and Qin C Z 2007 *Computers & Geosiences* **33** 952

[21] Pei T, Zhu A X, Zhou C H, Li B L and Qin C Z 2006 *Int. J. Geogr. Inf. Sci.* **20** 153

[22] Yang P, Hou W and Zhi R 2009 *Acta Phys. Sin.* **58** 2097 (in Chinese)

[23] Yang P, Feng G L, Liu W D, Wang Q G and Xiong K G 2010 *J. Appl. Meteorol. Sci.* **21** 319 (in Chinese)

[24] Lian Y and An G 1998 *Acta Meteorol. Sin.* **56** 724 (in Chinese)

[25] Karl T R, Kukla G, Razuvayev V, Changery M J, Quayle R G, Heim R R, Easterling D R and Fu C B 1991 *Geophy. Rev. Lett.* **18** 2253

[26] Chen H B and Fan X H 2009 *Climatic and Environmental Research* **14** 329 (in Chinese)

[27] Wang W, Zeng Z and Karl T R 1990 *Geophys. Res. Lett.* **17** 2377

[28] Klysik K and Fortuniak K 1999 *Atmos. Environ.* **33** 3885

[29] Zhang X G and Li X Q 1982 *Acta Meteorol. Sin.* **40** 198 (in Chinese)

[30] Wang Y N, He J H and Jiang A J 2009 *J. Tropical Meteorology* **25** 97 (in Chinese)

[31] Chen Y, Ren G Y, Wang L, Zhou X K and Zhang Q 2009 *J. Appl. Meteorol.* **20** 539 (in Chinese)

[32] Wang Y G, Gong Z S, Xu L and Ai X 2005 *Quarterly Journal of Applied Meteorology* **16** 85 (in Chinese)